Science Advances
AAAS

Manuscript Template

Title

- Lead Adsorbing Ionogel-based Encapsulation for Impact-Resistant, Stable and Lead-Safe Perovskite Modules

Short Title

- Stable and lead-safe perovskite modules

Authors

Xun Xiao,[1,#] Meixiang Wang,[2,#] Shangshang Chen,[1] Yihang Zhang,[3] Hangyu Gu,[1] Yehao Deng,[1] Guang Yang,[1] Chengbin Fei,[1] Bo Chen,[1] Yuze Lin,[3,4] Michael D. Dickey[2] Jinsong Huang[1,*]

Affiliations

[1] Department of Applied Physical Sciences, University of North Carolina, Chapel Hill, NC 27599, USA

[2] Department of Chemical and Biomolecular Engineering, North Carolina State University, Raleigh, NC 27695, USA

[3] Beijing National Laboratory for Molecular Sciences, CAS Key Laboratory of Organic Solids, Institute of Chemistry, Chinese Academy of Sciences, Beijing 100190, China

[4] University of Chinese Academy of Sciences, Beijing 100049, China

[#] These authors contributed equally.

*Corresponding author email: jhuang@unc.edu

Abstract

Despite the high efficiency and low-cost prospect for perovskite solar cells, great concerns of lead toxicity and instability remain for this technology. Here, we report an encapsulation strategy for perovskite modules based on lead-adsorbing ionogel, which prevents lead leakage and withstand long-term stability tests. The ionogel layers integrated on both sides of modules enhance impact resistance. The self-healable ionogel can prevent water permeation into the perovskite layer, and absorb lead that might leak. The encapsulated devices pass the Damp Heat and Thermal Cycling accelerated stability tests according to IEC 61215 standard. The ionogel encapsulation reduces lead leakage to undetectable level after the hail-damaged module is soaked in water for 24 hours. Even being rolled over by a car followed by water-soaking for 45 days, the ionogel encapsulation reduces lead leakage by three orders of magnitude. This work provides a strategy to address lead leakage and stability simultaneously for perovskite modules.

Teaser

An ionogel can defend impact damage and adsorb lead ions, which enhances the perovskite modules stability and reduces lead leakage when encountering damage.

MAIN TEXT

The manuscript should be a maximum of 15,000 words.

Introduction

Metal halide perovskites (MHP) have demonstrated great potential for next-generation low-cost and efficient solar cells.(*1-3*) The certified power conversion efficiencies (PCEs) have already exceeded 25% for single-junction perovskite solar cells (PSCs) and 29% for perovskite/silicon tandem solar cells.(*4, 5*) Meanwhile, large-area perovskite modules achieved a certified efficiency of 18.6% (area of 30-60 cm^2), which is comparable to that of commercialized silicon modules.(*6*) This suggests that the PCE is no longer a critical concern for commercialization of perovskite photovoltaics. Nevertheless, its real-world application has been greatly hindered with a concern that perovskites containing water-soluble lead may cause great potential pollution to soil and underground water resources. Toxic lead intake through water or food chains can accumulate in the human body, threatening human health, including brain damage, kidney and liver dysfunction, especially for children.(*7-9*) Therefore, diminishing the negative impact of lead from PSCs on the environment and human health needs to be completed before their large-scale commercialization.(*10*) One intuitive way is to replace lead perovskites with non-toxic compositions like tin (Sn)-perovskites, or double perovskites such as $Cs_2AgBiBr_6$.(*11, 12*) However, tin-based PSCs suffer from poor stability as Sn^{2+} could be easily oxidized to Sn^{4+}, even by the solvents that process tin-perovskites,(*13-15*) while the PCEs of double perovskites devices are too small to be considered as useful.(*16*) Despite its drawbacks, lead-containing perovskites are still the primary candidate to realize efficient and stable perovskite solar modules.

Alternative approaches have been recently explored to minimize lead leakage to the environment for lead-based PSCs.(*17, 18*) As components in efficient perovskite solar cells, charge transport layers, such as alkoxy-PTEG for hole transporting layer (HTL)(*18*) and a 2D metal-organic framework for electron transporting layer (ETL)(*19*), are naturally good candidates to trap lead without additional efforts. Nevertheless, charge transport layers usually have a relatively small thickness of ~20-50 nm to allow efficient charge collection(*18, 19*), which could not provide enough capacity to absorb lead ions from a typical 500-1000 nm-thick perovskite layer. Another method is to wrap the PSCs with physical barriers or lead absorbing materials to prevent lead from leakage. This includes self-healing polymer which physically blocks water permeation into devices even if the glass substrates break(*17*), or lead absorbing materials including a water-swelling lead-absorbing polymer or ion exchange resins to chemically capture lead from leakage by over 90% under simulated hail tests.(*20, 21*) However, the physical blocking polymer could only slow down the lead leakage speed, i.e. lead would eventually leak out. A lead-adsorbing layer coated on the front side would require a physical shield, otherwise, it might lose its functionality during the long-term exposure, i.e. metal ions from rainwater or dust would saturate the binding sites of the layer.(*22, 23*) Putting the lead absorber inside the perovskite layer nicely avoids this issue.(*24*) On the other hand, encapsulation is necessary to screen environmental stimuli to enhance operational stability of solar cells, which requires a distinct layer to protect perovskite devices.(*25-27*) Considering lead toxicity and instability in perovskite modules are equally essential, while they are now individually studied, an effective strategy is needed to solve both problems simultaneously to demonstrate stable and lead-safe perovskite photovoltaics a reliable product in real-world applications.

Another issue that has received very little attention is that standard tempered glass used for perovskite solar cell substrate or encapsulation can shatter when damaged. This may

dramatically boost the insurance for the installation of solar cells, limiting the wide adoption of the perovskite PV technology. Here, we report a self-healable, lead-adsorbing ionogel-based encapsulation for perovskite modules, which have multiple functions of enhancing impact resistivity, and reducing lead leakage, increasing the stability of perovskite modules. The ionogel sealants are coated on the surface of the front glass and between electrode and encapsulation glass, which can effectively suppress lead leakage from broken modules after hail test or compression by car wheels and soaking in water for 45 days. At the same time, the ionogel can hold the shattered glass together even if they are completely damaged. The fabricated perovskite mini-modules showed the highest performance including a high aperture efficiency of 18.5% for an area of 31.5 cm^2, and the resultant solar cells passed Damp Heat (DH) and Temperature Cycling (TC) IEC 61215 standards tests.

Results

Lead adsorbing ionogel synthesis

Ionogels have highly tunable optical, mechanical and chemical properties.(*28-30*) To endow it lead-adsorbing capability and decent mechanical properties, we synthesized the ionogel with lead-binding monomers of acrylic acid (AA), covalent crosslinker of methylene-bis-acrylamide (MBAA), thermo-initiator of azobisisobutyronitrile (AIBN) and ionic liquid of tributyl(methyl)phosphonium dimethyl phosphate (TPDP) whose chemical structures are shown in Fig. S1. The resultant poly-acrylic-acid (PAA) chains in the ionogel were covalently crosslinked by MBAA, forming a three-dimensional network swelling in TPDP (Fig. 1a). PAA hydrogels with PAA network swelling in water were commonly applied to anchor heavy metal ions with the carboxyl groups on PAA chains for water purification.(*31-34*) Replacing water (i.e. hydrogel) with non-volatile and thermal stable phosphonium ionic liquid (i.e. ionogel) not only makes the gel stable by suppressing solvent evaporation(*35*), but also provides more lead bonding sites with phosphate anions (Fig. 1a).(*36*) For the 100 μm-thick PAA ionogel, the amounts of phosphate groups of TPDP and carboxyl groups of PAA are about 0.175 mol m^{-2} and 0.555 mol m^{-2}, which can provide total lead binding sites of 0.365 mol m^{-2}, i.e. adsorbing lead up to 76.25 g m^{-2}. It is about 100 times larger than the lead amount (~3.5×10^{-3} mol m^{-2} or 0.73 g m^{-2}) in typical PSCs with a perovskite layer thickness of 500 nm.(*21*) The transparency of the PAA ionogel was investigated by coating a 500-μm thick ionogel onto a glass substrate. The transmissions (300–850 nm) of glass substrates with and without ionogel showed no difference (Fig. 1b). This allows the ionogel to be coated at the front light-incident surface of glass without reducing solar cell light-harvesting efficiency.

The ionogel Young's modulus was determined to be 69.95±3.08 MPa (Fig. S2a)(*37*), which is comparable to that of commercial ethylene vinyl acetate (EVA) and POE sealants.(*38, 39*) The ionogel could endure a strain of 500% without fracture (Fig. S3). The ionogel is highly stretchable, because the polymer networks are highly solvated in the ionic liquid and resulting in an elastic network. The adhesion property of the ionogel was demonstrated by attaching five metal balls (8.36 g for each) to an ionogel/glass substrate by hand, then flipped and shake the substrate for vibration (Movie S1). As shown in the movie, all five metal balls remained well-attached for the test, suggesting the excellent adhesion ability of the ionogel. The adhesion capability should come from the electrostatic interactions and Van der Waals interactions at the surface due to the charged polymer chains and solvent in ionogel. The robust and adhesive ionogel can provide mechanical protection for solar modules as an encapsulant. For demonstration, 1.1 mm-thick tempered glass and glass with a 500-μm thick ionogel attached were both hit by a metal ball (8.36 g) dropping from a height of 2 m (Fig.

1c and Movie S2). The bare glass was immediately shattered into pieces, while the glass with ionogel exhibited no obvious damage after one shot by the metal ball. After continuous 14 shots, the glass cracked, while the ionogel layer remained intact and held the broken glass pieces. This confirmed that introduction of ionogel layer would greatly enhance mechanical impact resistance. The substrate of broken glass with ionogel was then exposed to the ambient with average relative humidity of ~50%, temperature of ~23 °C for 85 days before re-checking the adhesion ability. As shown in Fig. S4, the ionogel could maintain well-adhesive to hold the broken glass pieces and be able to adhere to metal balls after the 85 days exposure, indicating its superior environmental stability. The UV stability of the ionogel was analyzed by exposing it to a UV light with an intensity of 120 W m^{-2} in wavelength of 280 to 360 nm range for 500 hours, where commercial polyolefin (POE) sealants were tested side by side for comparison (Fig. 1d). The total exposed UV dose was determined to be 60 kWh m^{-2}, surpassing the required exposure dose of 15 kWh m^{-2} in standard IEC 61215 UV Precondition Test or 50 kWh m^{-2} in IEC 62108 UV Conditioning Test.(*40*) Both ionogel and POE samples were shown to be UV stable with less than 1% transmission loss after exposure. The ionogel has a moderate cost compared to other sealants (Fig. S5 and Supplementary Note 1). Besides, the ionogel has excellent self-healing property. As demonstrated in Fig. 1e, two dog-bone shape ionogel samples were dyed to blue and black, respectively, and cut completely in the middle. Two pieces from different pristine samples were put together and healed at 50 ˚C (solar module working temperature) for 2 h. The self-healed sample was then able to remain intact with a strain of >250% (Fig. 1e & Fig. S2b). The self-healing property may come from the abundant reversible hydrogen bonds between -COOH groups on polymer chains in the networks that could be easily re-formed at elevated temperature and then act as physical crosslinkers. This would allow self-repairing of cracks in the lead adsorbing layer when undergoing extreme impact, maintaining its mechanical integrity and blocking lead leakage.

The capability and kinetics of the PAA ionogel to capture lead leakage from perovskite devices were investigated by soaking PAA ionogel film into methylammonium lead iodide ($MAPbI_3$) aqueous solution and sampling at different time to determine temporal lead concentration in the solution. Note that, if Pb^{2+} ions from typical perovskite devices were completely dissolved by rainwater in North Carolina, lead concentration of the contaminated rainwater would be 0.57 ppm (Method).(*41*) Here, we simulated a much worse scenario by soaking a ~20 cm^2, 100-μm thick PAA ionogel film into 50 mL of 8.6×10^{-4} M $MAPbI_3$ solution (~178 ppm Pb^{2+}), which corresponded to a lead amount from a 500 nm thick perovskite layer with 121.9 cm^2 in area. As shown in Fig. 1f, most Pb^{2+} ions were absorbed within 10 minutes. The adsorption kinetics were fitted by pseudo-first-order model and pseudo-second-order model based on data before the equilibrium was reached, respectively (inset in Fig. 1e and Fig. S6).(*42*) The better fitting from pseudo-second-order model with R^2 of 0.927 (Supplementary Table 1) suggested the rate-limiting step is chemical sorption(*43*), which is consistent with previous studies about PAA adsorbing metal ions from aqueous solution.(*31, 44*) Hence, the fast adsorption should benefit from swelling of ionogel in water which increases the absorbing surface area. The adsorption isotherm was conducted and fitted with Langmuir model (Fig. S7), suggesting a maximum lead adsorption capacity of 1.31 mmol g^{-1} and diffusion coefficient (K_d) of 8.05 L g^{-1}.

Device performance with ionogel based encapsulation

To validate the compatibility of the ionogel with efficient and stable perovskite solar cells and mini-modules, we incorporated the PAA ionogel into the perovskite devices encapsulation with a structure of polydimethylsiloxane (PDMS) anti-reflection/ionogel-1/indium tin oxide (ITO) glass/poly(bis(4-phenyl)(2,4,6-trimethylphenyl)amine)

(PTAA)/perovskite (500-1000 nm)/C_{60}/bathocuproine (BCP)/copper (Cu)/ POE /ionogel-2/glass cover (Fig. 2a), and used silicone glue for edge sealing. The top anti-reflection PDMS layer could enhance light trapping and protect the lead-adsorbing ionogels from contamination. The 100 μm-thick ionogel layers on the top and bottom sides help to provide mechanical impact resistivity and lead adsorbing capacity. The POE layer provides encapsulation and separate ionogel and perovskite devices, while the bottom cover with heat-strengthened glass further enhances mechanical integrity (Supplementary notes 2).

A mixed methylammonium (MA^+)/formamidinium (FA^+) lead iodide perovskite of $MA_{0.7}FA_{0.3}PbI_3$ was applied to achieve perovskite solar cells with high efficiency and excellent reproducibility.(*45*) The produced champion mini-module before encapsulation with an aperture area of 31.5 cm^2 exhibited a *PCE* of 17.2% with a short circuit current (I_{SC}) of 72.54 mA, open circuit voltage (V_{OC}) of 9.89 V and fill factor (*FF*) of 0.753 (Fig. 2b). *PCE* was enhanced to of 18.5% with a I_{SC} of 74.6 mA, V_{OC} of 10.09 V and *FF* of 0.773 after the encapsulation. The current increase should be from introduction of anti-reflection layer, while the V_{OC} and FF enhancement might result from additional thermal annealing induced defect healing when curing ionogel. It indicated the encapsulation could help to suppress releasing of decomposition products like CH_3NH_2 and I_2 under thermal annealing, which commonly occurs upon heating devices without a good encapsulant.(*27, 46*) A J_{SC} enhancement was observed for small area PSCs with a champion efficiency of 22.9% after encapsulation. The statistic results from 32 PSCs showed an improvement from 20.9±0.98% to 21.7±0.93% (Fig. 2d and Fig. S8), which further confirmed that the compatibility and reproducibility of ionogel-based encapsulation with high efficiency PSCs.

The long-term stability of the ionogel-based encapsulated devices was validated with damp heat and thermal cycling tests according to IEC 61215 accelerated tests standard.(*27, 47*) It is required to withstand the moisture ingress and temperature extremes for a certain test duration (>1000 hours for DH, 200 cycles for TC) for commercializing a photovoltaic technology.(*27*) A device structure of ITO/PTAA/$FA_{0.92}Cs_{0.08}PbI_3$/C_{60}/SnO_2/Cu/ITO with more stable perovskite composition and robust charge collection layers was applied to verify the compatibility of this encapsulation strategy.(*6*) For DH test, five encapsulated devices with an average initial efficiency of 17.5±0.55% were exposed to an environment with 85% relative humidity at 85 ˚C for over 1000 hours. The device efficiencies were checked every 72 hours during the test. The averaged efficiency retained 95.2% of initial values after 1000 h test (Fig. 2e). Another batch of PSCs with an average efficiency of 17.8±0.78% were applied to TC test, i.e. the temperature of the devices was cycled from -40 ˚C and 80 ˚C. The temperature evolution of one cycle was provided in Fig. S9. After 210 cycles, the devices retained 96.1% of their initial efficiency, exceeding the IEC 61215 standard requirement (Fig. 2f).(*25, 26, 47*) These results conclude that the ionogel-based encapsulation can provide the protection that is needed to achieve the long-term stability of PSCs, which should benefit from suitable Young's modulus and superior thermal stability of the sealants and self-healing capability of ionogel.

Lead leakage against hail test

We studied how effective the encapsulation with PAA ionogel prevents lead leakage from damaged solar mini-modules. The $MA_{0.7}FA_{0.3}PbI_3$ perovskite solar mini-modules with area of 52.7±3.2 cm^2 and the structure of ITO/PTAA/$MA_{0.7}FA_{0.3}PbI_3$/C_{60}/BCP/Cu were fabricated in one batch to avoid sample variation. The mini-modules were then encapsulated by POE or ionogel with structures shown in Fig. 3a, named as structure A, B and C respectively. In structure A, a typical encapsulation strategy for thin film photovoltaics was applied(*48*), i.e. perovskite solar modules were encapsulated by 1.1 mm-thick tempered

glass with POE at the bottom side and silicone glue for edge sealing, while no encapsulation was performed on the top sides. Encapsulation for both top and bottom sides like silicon solar panels were adopted in structure B for comparison.(*49*) In structure C, we incorporated lead-adsorbing ionogel layers into encapsulation at top and bottom sides for lead leakage study. To simulate extreme hail impact, a metal ball with weight of ~ 64 g, diameter of 1 inch was dropped from 2 m height to hit the suspended perovskite solar mini-modules with various encapsulation methods (Movie S3), following the FM 44787 standard testing.(*50*)

When encountering the metal ball, mini-modules with structure A shattered into pieces, while mini-modules with structures B and C remained intact with typical star-shape cracks at the impact position (Movie S3). It suggests the critical role of top-side encapsulation. The damaged perovskite solar mini-modules were then soaked in the deionized (DI) water to assess the lead leakage status, simulating the worst scenario of the damaged modules were flooded. Each damaged module was soaked with 200 mL DI water in a Petri dish as shown in the inset of Fig. 3b. The contaminated water was sampled after varied soaking durations, then measured with inductively coupled plasma mass spectrometry (ICP-MS) to determine the lead concentration and temporal leakage amount (Fig. 3b). Modules packaged with POE showed a quick lead leakage with a dramatic increase of lead concentration in contaminated water to respective 6.23±0.39 ppm and 5.71±0.17 ppm for structure A and B in the first 2 hours, which might be from the water fast flushing into the cracks or exposed area in the device and encapsulation layer. This is evidenced by the quick color change at the cracks from black to yellow of the damaged modules with structures A and B (Fig. 3c-d).(*51*) After that, the contaminated lead concentration gradually increased to 10.65±0.59 ppm with structure A and 8.38±0.38 ppm with structure B when the water-soaking time reached 24 hours, which corresponds to a cumulated lead leakage of 0.4±0.02 and 0.32±0.01 g m^{-2}, respectively. This might be caused by water permeation into the perovskite layer because the yellow regions expanded in both modules. In striking contrast, contaminated DI water after 24 hours soaking of the damaged mini-module with ionogel incorporated structure C encapsulation exhibited lead concentration of 0.63±0.18 ppb (corresponding to a lead leakage of 24±6.8 μg m^{-2}), which was below instrument detection limit (1 ppb) and consistent with no color change of the modules (Fig. 3e). It indicated that one shot of metal ball on the surface could not effectively damage the encapsulated mini-modules with structure C to create path for water permeation into perovskite layer through the cracks. This agrees with the robust mechanical protection from ionogel that defends the impact. Water dripping test to simulate rainfall was conducted over the damaged minimodules. The DI water was dripped onto the top surface of broken modules with a rate of 5 mL h^{-1} for 1 hour, corresponding to a 50 mm h^{-1} rainfall. The resultant water was collected and tested by ICP-MS to determine the lead leakage amount. The lead concentrations in the contaminated water were 12.96±0.70 ppm, 0.63±0.29 ppb and 0.48±0.22 ppb for structure A, B and C respectively (Fig. S10). The suppressed lead leakage in structure B and C for water dripping test should come from the protection from top-side encapsulation, as water would mainly travel along the top surface. It is noted that the structure used here is glass/perovskite/glass package without using a backsheet. If a polymer backsheet is used, like in regular non-bifacial silicon modules, the lead leakage from backside would be much less. The difference of water dripping test and soaking test would not be as large as seen here.

Lead leakage against car rolling

Apart from enhanced mechanical impact resistance, the robust ionogel in structure C was expected to serve as lead adsorbing materials to further reduce lead leakage. That is, when the substrates are severely cracked and water penetrates into the perovskite layer, the robust, stretchable and self-healable ionogel layer would maintain its mechanical integrity and

adsorb lead from leakage (Fig. S11). The high destructive hail test with an impact density of 1 impact per square inch (i.e. 8 impacts for modules used here) was then conducted to simulate severe hailstorm. Similar trends of a quick color change followed by an extended yellowing were observed in structure A and B under the destructive tests (Fig. S12). The cumulated lead leakage reached 0.60 and 0.47 g m^{-2} for structure A and B respectively (Fig. S13). For module in structure C, color change was observed at the edge from 3 hours soaking. It indicated water penetrated into the perovskite layer. However, the accumulated lead leakage amount in the soaking water did not show a significantly increase with a final value of 7.8×10^{-5} g m^{-2}, which was four orders of magnitude less than that in structure A.

To simulate another extreme scenario, a bare ~ 1 μm thick perovskite film on glass substrates (2×3 inches) was encapsulated by ionogel with a similar stacking structure of A, B and C shown in Fig 3a. The encapsulated films were placed on the ground and rolled over twice with a car (>1500 kg) to damage the modules (Fig. 4a & Movie S4). Perovskite films encapsulated with structure A exhibited obvious cracks after the car rolling, compared with films packaged with structure B and C (Fig. 4). Water-soaking test were then applied to assess the lead leakage (Fig. 4b). Both A and B with POE as encapsulant showed a quick lead escape during water soaking in the first 10 days, and then gradually increased after 45 days soaking, which could also be identified from the corresponding color change of the perovskite films in Fig. 4 c-d. While for the ionogel based structure C, the encapsulated film did not exhibit notable color change (Fig. 4e), and showed negligible lead leakage for the first 5 days soaking, which should result from suppressed water permeation rate due to less cracks with strong mechanical protect. At around 10 days soaking, the film started to change color, indicating water penetrated into the perovskite layer and induced decomposition. The area with yellow color expanded in the following 35 days. In contrast to perovskite films encapsulated with A and B, the color change of the film only happened at the edge after long time soaking (>10 days) and did not correspond to a quick rise in lead concentration of the contaminated water. This should be from the water permeation through device edges to perovskite layer, while filtering effect of lead-adsorbing ionogel layer that trapped most lead ions in the path of water penetration. The resultant lead concentrations after 45 days soaking were 13.6±0.85 ppm, 10.7±0.65 ppm and 0.013±0.0025 ppm for perovskite films encapsulated with structure A, B and C respectively, which corresponds to accumulated lead leakage of 0.7±0.04, 0.55±0.034 g m^{-2} and 0.67±0.13 mg m^{-2}. It suggests a lead leakage reduction by almost three orders of magnitude when adopting encapsulation with ionogel based structure C compared to POE-based structure A. We also compared the lead adsorption and device performance in structure C with previous reports (Table 1): perovskite devices with the ionogel-based encapsulation exhibit both effective lead leakage reduction as well as impressive device efficiency and stability.

Discussion

In summary, we report a tough, self-healable and lead-adsorbing ionogel to be incorporated into perovskite solar modules encapsulation to reduce lead leakage and enhance device stability simultaneously. The ionogel-based encapsulation is compatible for PSCs with high efficiency (champion PCE of 18.5 % for mini-module and 22.9 % for small cells) and shows impressive long-term stability (less than 5% relative efficiency loss after Damp Heat and Thermal Cycling tests). More importantly, incorporation of ionogel in the encapsulation dramatically suppressed lead leakage from broken perovskite modules. Undetectable lead (<1 ppb) could escape from the damaged perovskite module after a simulated hail test followed by water soaked for 24 hours. Even under extreme conditions like being run over by a car, the robust ionogel layer-based encapsulation could remain intact and act as a filter layer to suppress lead leakage by almost three orders of magnitude better compared to

devices encapsulated by the standard glass cover and POE sealant. These results will accelerate perovskite solar technology to real world applications.

Materials and Methods

Materials: The materials were used as follows: acrylic acid (AA) (anhydrous, 99%, Sigma Aldrich), tributyl(methyl)phosphonium dimethyl phosphate (TPDP) (95%, Synthonix), azobisisobutyronitrile (AIBN) (Sigma Aldrich), methylene-bis-acrylamide (MBAA) (Sigma Aldrich). All materials are used as received without further purification.

Preparation of PAA ionogel: The ionogel was synthesized using a one-step method by polymerizing AA monomers in TPDP. In a typical procedure, 0.001 g MBAA and 0.001 g AIBN were firstly dissolved in 0.4 g AA monomer MBAA and AIBN are each 0.25 wt% relative to AA. Then 0.6 g TPDP was mixed in to form a homogeneous solution. The precursor was then inserted into designed molds and heated up to 80 °C for 15 mins in glovebox to obtain the ionogel.

POE encapsulation: The encapsulation with POE film was conducted by hot-pressing under vacuum condition. The film was heated to 140 °C for 10 mins and pressed for encapsulation.

Tensile tests: The tensile properties were measured using a tensile-compressive tester (Instron 5943). The samples with dog bone-shape (length: 35 mm, width: 2 mm and gauge length: 12 mm) were used in the tensile tests with a speed of 100 mm min^{-1} following standards. The fracture strength was defined as the nominal stress at failure. The Young's modulus was defined as the slope of the tensile stress-strain curves.

Self-healing test: Two dog-bone-shaped samples (dyed blue and black) were cut into two halves and then the cut surfaces of the blue and black pieces were healed at 50 ˚C for 2 h. The tensile stress-strain curves of the healed samples were recorded by the Instron.

Lead adsorption test: For adsorption kinetics tests, 0.2 g PAA ionogel were added into 50 mL of 8.6×10^{-4} M $MAPbI_3$ aqueous solution with constant stirring with an agitation speed of 120 r.p.m. Samples were extracted from the reaction mixture with different delay time. The samples were analyzed by an ICP-MS Nexion 300D to determine the lead concentration. The absorbed lead amount per unit mass at time t, q_t, was calculated by $q_t = \frac{(C_0-C_t)V}{m}$, wherein C_0 is the initial concentration and C_t is the concentration at time t, V is the volume of the solution (0.05 L), m is the adsorbant mass (0.2 g).

Estimate lead leakage by rainwater in North Carolina: The average annual precipitation in North Carolina is 1279 mm, which corresponds to rainwater of 127.9 mL cm^{-2}. The lead concentration is 0.73 g m^{-2} for a typical 500 nm thick perovskite layer, considering the density of 4.16 g cm^{-3} in $MAPbI_3$. Hence, the lead concentration of contaminated rainwater should be 0.57 mg L^{-1} or 0.57 ppm, if all lead could be dissolved in rainwater.

References

1. A. Kojima, K. Teshima, Y. Shirai, T. Miyasaka, Organometal halide perovskites as visible-light sensitizers for photovoltaic cells. *Journal of the American Chemical Society* **131**, 6050-6051 (2009).
2. M. Liu, M. B. Johnston, H. J. Snaith, Efficient planar heterojunction perovskite solar cells by vapour deposition. *Nature* **501**, 395-398 (2013).
3. X. Zheng, B. Chen, J. Dai, Y. Fang, Y. Bai, Y. Lin, H. Wei, X. C. Zeng, J. Huang, Defect passivation in hybrid perovskite solar cells using quaternary ammonium halide anions and cations. *Nature Energy* **2**, 17102 (2017).
4. NREL Best Research-Cell Efficiencies. *https://www.nrel.gov/pv/cell-efficiency. html*, (2020).

5. A. Al-Ashouri, E. Köhnen, B. Li, A. Magomedov, H. Hempel, P. Caprioglio, J. A. Márquez, A. B. M. Vilches, E. Kasparavicius, J. A. Smith, Monolithic perovskite/silicon tandem solar cell with> 29% efficiency by enhanced hole extraction. *Science* **370**, 1300-1309 (2020).
6. Y. Deng, S. Xu, S. Chen, X. Xiao, J. Zhao, J. Huang, Defect Compensation in Formamidinium-Cesium Perovskites for Highly Efficient and Stable Solar Modules. *Nature Energy* **6,** 633–641 (2021).
7. A. Rajagopal, K. Yao, A. K. Y. Jen, Toward perovskite solar cell commercialization: a perspective and research roadmap based on interfacial engineering. *Advanced Materials* **30**, 1800455 (2018).
8. M.-G. Ju, M. Chen, Y. Zhou, J. Dai, L. Ma, N. P. Padture, X. C. Zeng, Toward eco-friendly and stable perovskite materials for photovoltaics. *Joule* **2**, 1231-1241 (2018).
9. R. M. Harrison, D. Laxen, Lead pollution. *Causes and control. Chapman and Hall, London*, (1981).
10. Z. Shi, J. Guo, Y. Chen, Q. Li, Y. Pan, H. Zhang, Y. Xia, W. Huang, Lead-free organic–inorganic hybrid perovskites for photovoltaic applications: recent advances and perspectives. *Advanced Materials* **29**, 1605005 (2017).
11. W. Ke, M. G. Kanatzidis, Prospects for low-toxicity lead-free perovskite solar cells. *Nature communications* **10**, 965 (2019).
12. P. V. Kamat, J. Bisquert, J. Buriak, Lead-free perovskite solar cells. *ACS Energy Letters* **2**, 904-905 (2017).
13. E. W.-G. Diau, E. Jokar, M. Rameez, Strategies to improve performance and stability for tin-based perovskite solar cells. *ACS Energy Letters* **4**, 1930-1937 (2019).
14. M. I. Saidaminov, I. Spanopoulos, J. Abed, W. Ke, J. Wicks, M. G. Kanatzidis, E. H. Sargent, Conventional solvent oxidizes Sn (II) in perovskite inks. *ACS Energy Letters* **5**, 1153-1155 (2020).
15. J. Pascual, G. Nasti, M. H. Aldamasy, J. A. Smith, M. Flatken, N. Phung, D. Di Girolamo, S.-H. Turren-Cruz, M. Li, A. Dallmann, Origin of Sn (ii) oxidation in tin halide perovskites. *Materials Advances* **1**, 1066-1070 (2020).
16. C. Wu, Q. Zhang, Y. Liu, W. Luo, X. Guo, Z. Huang, H. Ting, W. Sun, X. Zhong, S. Wei, The dawn of lead-free perovskite solar cell: highly stable double perovskite Cs2AgBiBr6 film. *Advanced Science* **5**, 1700759 (2018).
17. Y. Jiang, L. Qiu, E. J. Juarez-Perez, L. K. Ono, Z. Hu, Z. Liu, Z. Wu, L. Meng, Q. Wang, Y. Qi, Reduction of lead leakage from damaged lead halide perovskite solar modules using self-healing polymer-based encapsulation. *Nature Energy* **4**, 585-593 (2019).
18. J. Lee, G. W. Kim, M. Kim, S. A. Park, T. Park, Nonaromatic Green-Solvent-Processable, Dopant-Free, and Lead-Capturable Hole Transport Polymers in Perovskite Solar Cells with High Efficiency. *Advanced Energy Materials* **10**, 1902662 (2020).
19. S. Wu, Z. Li, M.-Q. Li, Y. Diao, F. Lin, T. Liu, J. Zhang, P. Tieu, W. Gao, F. Qi, 2D metal–organic framework for stable perovskite solar cells with minimized lead leakage. *Nature Nanotechnology* **15**, 934-940 (2020).
20. S. Chen, Y. Deng, H. Gu, S. Xu, S. Wang, Z. Yu, V. Blum, J. Huang, Trapping lead in perovskite solar modules with abundant and low-cost cation-exchange resins. *Nature Energy* **5**, 1003-1011 (2020).
21. X. Li, F. Zhang, H. He, J. J. Berry, K. Zhu, T. Xu, On-device lead sequestration for perovskite solar cells. *Nature* **578**, 555-558 (2020).
22. N. Y. Hasan, D. Driejana, A. Sulaeman, Composition of Ions and Trace Metals in Rainwater in Bandung City, Indonesia. *IPTEK Journal of Proceedings Series* **3**, (2017).
23. Á. Keresztesi, I.-A. Nita, M.-V. Birsan, Z. Bodor, R. Szép, The risk of cross-border pollution and the influence of regional climate on the rainwater chemistry in the Southern Carpathians, Romania. *Environmental Science and Pollution Research*, 1-21 (2020).

24. S. Chen, Y. Deng, X. Xiao, S. Xu, P. N. Rudd, J. Huang, Perovskites in Mesoporous Lead Adsorbents for Non-Toxic Solar Modules. *Nature Sustainability* **4,** 636–643 (2021).
25. L. Shi, T. L. Young, J. Kim, Y. Sheng, L. Wang, Y. Chen, Z. Feng, M. J. Keevers, X. Hao, P. J. Verlinden, Accelerated lifetime testing of organic–inorganic perovskite solar cells encapsulated by polyisobutylene. *ACS applied materials & interfaces* **9**, 25073-25081 (2017).
26. R. Cheacharoen, C. C. Boyd, G. F. Burkhard, T. Leijtens, J. A. Raiford, K. A. Bush, S. F. Bent, M. D. McGehee, Encapsulating perovskite solar cells to withstand damp heat and thermal cycling. *Sustainable Energy & Fuels* **2**, 2398-2406 (2018).
27. L. Shi, M. P. Bucknall, T. L. Young, M. Zhang, L. Hu, J. Bing, J. Kim, T. Wu, N. Takamure, D. R. McKenzie, Gas chromatography–mass spectrometry analyses of encapsulated stable perovskite solar cells. *Science*, **368**, eaba2412 (2020).
28. D. Khodagholy, V. F. Curto, K. J. Fraser, M. Gurfinkel, R. Byrne, D. Diamond, G. G. Malliaras, F. Benito-Lopez, R. M. Owens, Organic electrochemical transistor incorporating an ionogel as a solid state electrolyte for lactate sensing. *Journal of Materials Chemistry* **22**, 4440-4443 (2012).
29. M. A. Firestone, M. L. Dietz, S. Seifert, S. Trasobares, D. J. Miller, N. J. Zaluzec, Ionogel-Templated Synthesis and Organization of Anisotropic Gold Nanoparticles. *Small* **1**, 754-760 (2005).
30. Z. Song, L. Li, D. Zhu, L. Miao, H. Duan, Z. Wang, W. Xiong, Y. Lv, M. Liu, L. Gan, Synergistic design of a N, O co-doped honeycomb carbon electrode and an ionogel electrolyte enabling all-solid-state supercapacitors with an ultrahigh energy density. *Journal of Materials Chemistry A* **7**, 816-826 (2019).
31. M. Q. Al-Abachi, N. S. Al-Awady, A. M. Al-Anbakey, Evaluation of poly acrylic acid (PAA) hydrogel beads as adsorbent for the removal of lead (II) ion from water. *Al-Nahrain Journal of Science* **16**, 30-39 (2013).
32. M. Zhang, L. Song, H. Jiang, S. Li, Y. Shao, J. Yang, J. Li, Biomass based hydrogel as an adsorbent for the fast removal of heavy metal ions from aqueous solutions. *Journal of Materials Chemistry A* **5**, 3434-3446 (2017).
33. Q. Meng, B. Peng, C. Shen, Synthesis of F127/PAA hydrogels for removal of heavy metal ions from organic wastewater. *Colloids and Surfaces B: Biointerfaces* **167**, 176-182 (2018).
34. G. Zhou, J. Luo, C. Liu, L. Chu, J. Crittenden, Efficient heavy metal removal from industrial melting effluent using fixed-bed process based on porous hydrogel adsorbents. *Water research* **131**, 246-254 (2018).
35. L. Zhu, J. Qiu, E. Sakai, A high modulus hydrogel obtained from hydrogen bond reconstruction and its application in vibration damper. *RSC advances* **7**, 43755-43763 (2017).
36. E. M. Martinis, P. Bertón, J. C. Altamirano, U. Hakala, R. G. Wuilloud, Tetradecyl (trihexyl) phosphonium chloride ionic liquid single-drop microextraction for electrothermal atomic absorption spectrometric determination of lead in water samples. *Talanta* **80**, 2034-2040 (2010).
37. M. X. Wang, Y. M. Chen, Y. Gao, C. Hu, J. Hu, L. Tan, Z. Yang, Rapid self-recoverable hydrogels with high toughness and excellent conductivity. *ACS applied materials & interfaces* **10**, 26610-26617 (2018).
38. M. Alexandre, G. Beyer, C. Henrist, R. Cloots, A. Rulmont, R. Jérôme, P. Dubois, Preparation and properties of layered silicate nanocomposites based on ethylene vinyl acetate copolymers. *Macromolecular rapid communications* **22**, 643-646 (2001).
39. F.-C. Chiu, S.-M. Lai, Y.-L. Chen, T.-H. Lee, Investigation on the polyamide 6/organoclay nanocomposites with or without a maleated polyolefin elastomer as a toughener. *Polymer* **46**, 11600-11609 (2005).

40. M. D. Kempe, in *2008 33rd IEEE Photovoltaic Specialists Conference*. (IEEE, 2008), pp. 1-6.
41. Average Annual Precipitation by State. *https://www.currentresults.com/Weather/US/average-annual-state-precipitation.php*, (2021).
42. R. Xiao, J. M. Tobin, M. Zha, Y.-L. Hou, J. He, F. Vilela, Z. Xu, A nanoporous graphene analog for superfast heavy metal removal and continuous-flow visible-light photoredox catalysis. *Journal of Materials Chemistry A* **5**, 20180-20187 (2017).
43. Y.-S. Ho, G. McKay, Pseudo-second order model for sorption processes. *Process biochemistry* **34**, 451-465 (1999).
44. N. Li, R. Bai, Highly enhanced adsorption of lead ions on chitosan granules functionalized with poly (acrylic acid). *Industrial & engineering chemistry research* **45**, 7897-7904 (2006).
45. S. Chen, X. Xiao, H. Gu, J. Huang, Iodine reduction for reproducible and high-performance perovskite solar cells and modules. *Science Advances* **7**, eabe8130 (2021).
46. S. Wang, Y. Jiang, E. J. Juarez-Perez, L. K. Ono, Y. Qi, Accelerated degradation of methylammonium lead iodide perovskites induced by exposure to iodine vapour. *Nature Energy* **2**, 16195 (2016).
47. P. Holzhey, M. Saliba, A full overview of international standards assessing the long-term stability of perovskite solar cells. *Journal of Materials Chemistry A* **6**, 21794-21808 (2018).
48. T. M. Shimpi, C. Moffett, W. S. Sampath, K. L. Barth, Materials selection investigation for thin film photovoltaic module encapsulation. *Solar Energy* **187**, 226-232 (2019).
49. S. Jiang, K. Wang, H. Zhang, Y. Ding, Q. Yu, Encapsulation of PV modules using ethylene vinyl acetate copolymer as the encapsulant. *Macromolecular Reaction Engineering* **9**, 522-529 (2015).
50. Approval Standard for Rigid Photovoltaic Modules (FM 44787). *www.fmapprovals.com/products-we-certify/understanding-the-benefits/fm-approved-photovoltaic-modules*, (2021).
51. B. Hailegnaw, S. Kirmayer, E. Edri, G. Hodes, D. Cahen, Rain on methylammonium lead iodide based perovskites: possible environmental effects of perovskite solar cells. *The journal of physical chemistry letters* **6**, 1543-1547 (2015).

Acknowledgments

Funding: We thank the financial support from National Science Foundation under award DMR-1903981. X.X. thanks the support by Dissertation Completion Fellowship from UNC Graduate School.

Author contributions: J.H. M.D. M.W. and X.X. conceived the idea. X.X. and M.W. synthesized the ionogel. X.X. conducted the encapsulation and lead leakage tests. M.W. and M.D. conducted mechanical properties tests. S.C. H.G. Y.D. G.Y. C.F. B.C. fabricated the perovskite modules and films. Y.Z. and Y.L. carried out the UV stability test. X.X. and J.H. wrote the paper. All authors reviewed the paper.

Competing interests: The authors declare no competing interests.

Data and materials availability: All data needed to evaluate the conclusions in the paper are present in the paper and/or the Supplementary Materials.

Fig.s and Tables

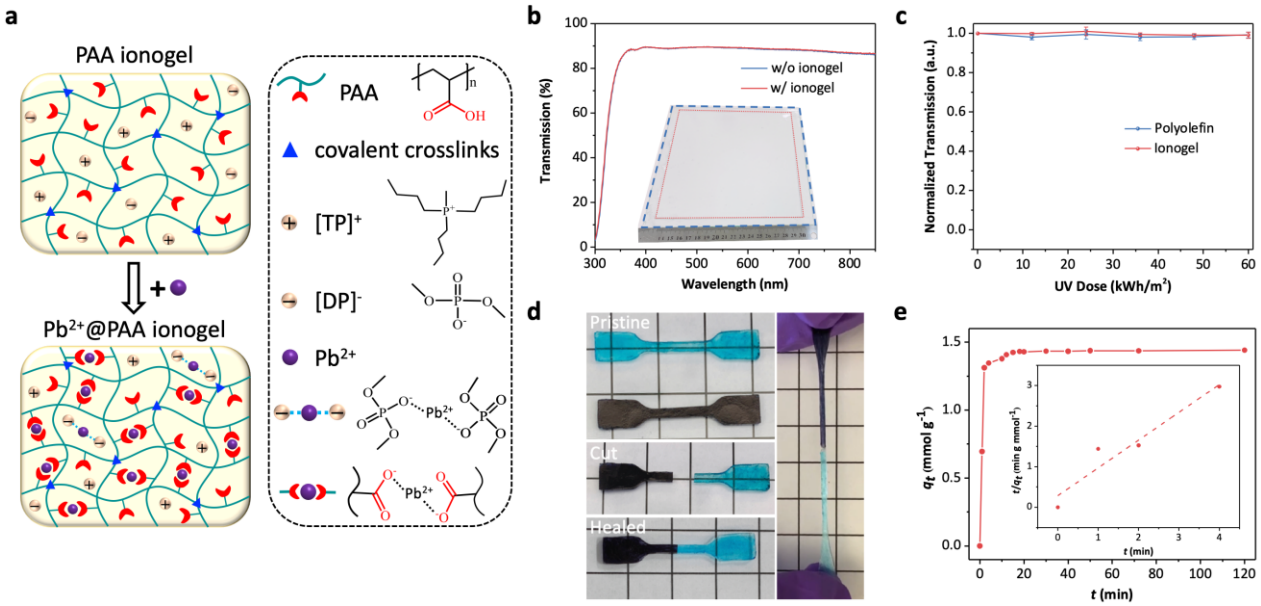

Fig. 1. Lead adsorbing ionogels. a, scheme of ionogel microstructure and lead adsorption mechanism; **b**, transmission of glass substrate with and without ionogel (thickness of 500 μm), inset is the image of ionogel with area of 15×15 cm^2 (indicated by red dash line) on glass substrate (indicated by blue dash line); **c**, substrates of bare glass and glass with ionogel hit by a metal ball (8.36 g) dropped from a height of 2 m; **d**,UV stability of ionogel and polyolefin, error bar from three independent tests; **e**, pristine ionogel samples dyed with different colors (left top); images of cut samples (left middle) and healed at 50 ˚C for 2 h (left bottom); image of a stretched healed sample (right), the square (1×1 cm^2) in the image could be the scale reference; **f**, lead adsorption kinetics of ionogel. Inset is kinetics fitting curve from a pseudo-second-order model with equation of $\frac{t}{q_t} = 1/(kq_e)^2 + \frac{t}{q_e}$, where k is the rate constant, q_e and q_t are absorbed lead ions at equilibrium and time t. Photo credit: Xun Xiao, University of North Carolina Chapel Hill.

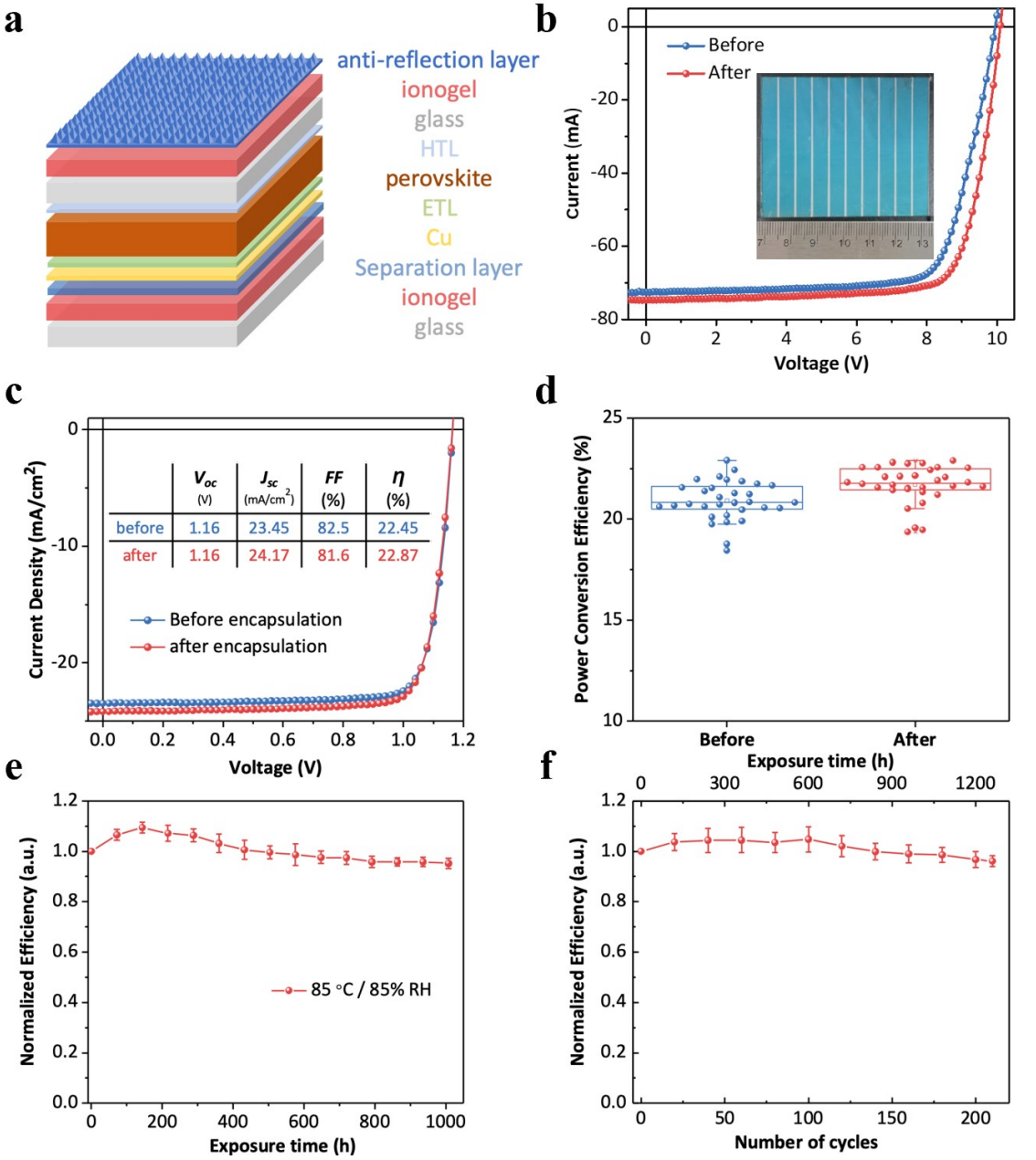

	V_{oc} (V)	J_{sc} (mA/cm^2)	FF (%)	η (%)
before	1.16	23.45	82.5	22.45
after	1.16	24.17	81.6	22.87

Fig. 2. Performance of ionogel encapsulated minimodules. a, device structure; **b**, *I-V* curves of perovskite module (area of 31.5 cm^2) before and after ionogel encapsulation, inset is the image of the encapsulated module; **c**, *J-V* curves of typical perovskite solar cells (area of 0.08 mm^2) before and after ionogel encapsulation, inset is the chart of parameters comparison; **d**, statistic results of efficiency distribution of 32 perovskite solar cells before and after ionogel encapsulation; **e-f**, efficiency evolution of perovskite solar cells during Damp Heat **(e)** and Thermal Cycling **(f)** tests according to IEC 61215 standard, error bars from statistic results of 5 independent devices. Photo credit: Xun Xiao, University of North Carolina Chapel Hill.

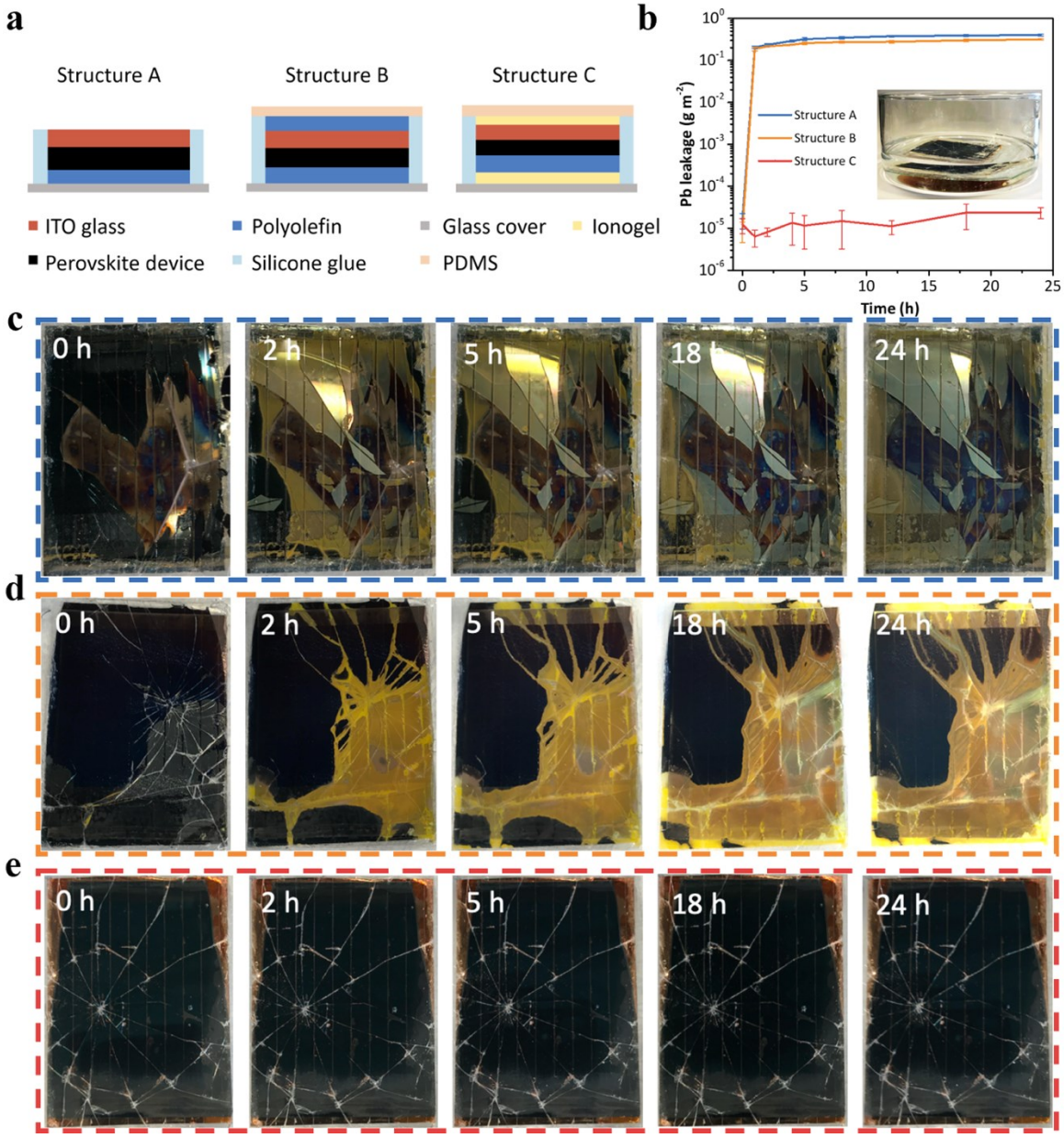

Fig. 3. Lead leakage of damaged mini-modules against metal ball falling. a, scheme of three encapsulation structures; **b**, water soaking test results for damaged mini-modules, inset is the image of the broken module soaking in DI water, error bar from three independent tests; **c-e**, typical evolution images of damaged perovskite modules with different encapsulation soaking in DI water for structure A (c), B (d) and C (e). Photo credit: Xun Xiao, University of North Carolina Chapel Hill.

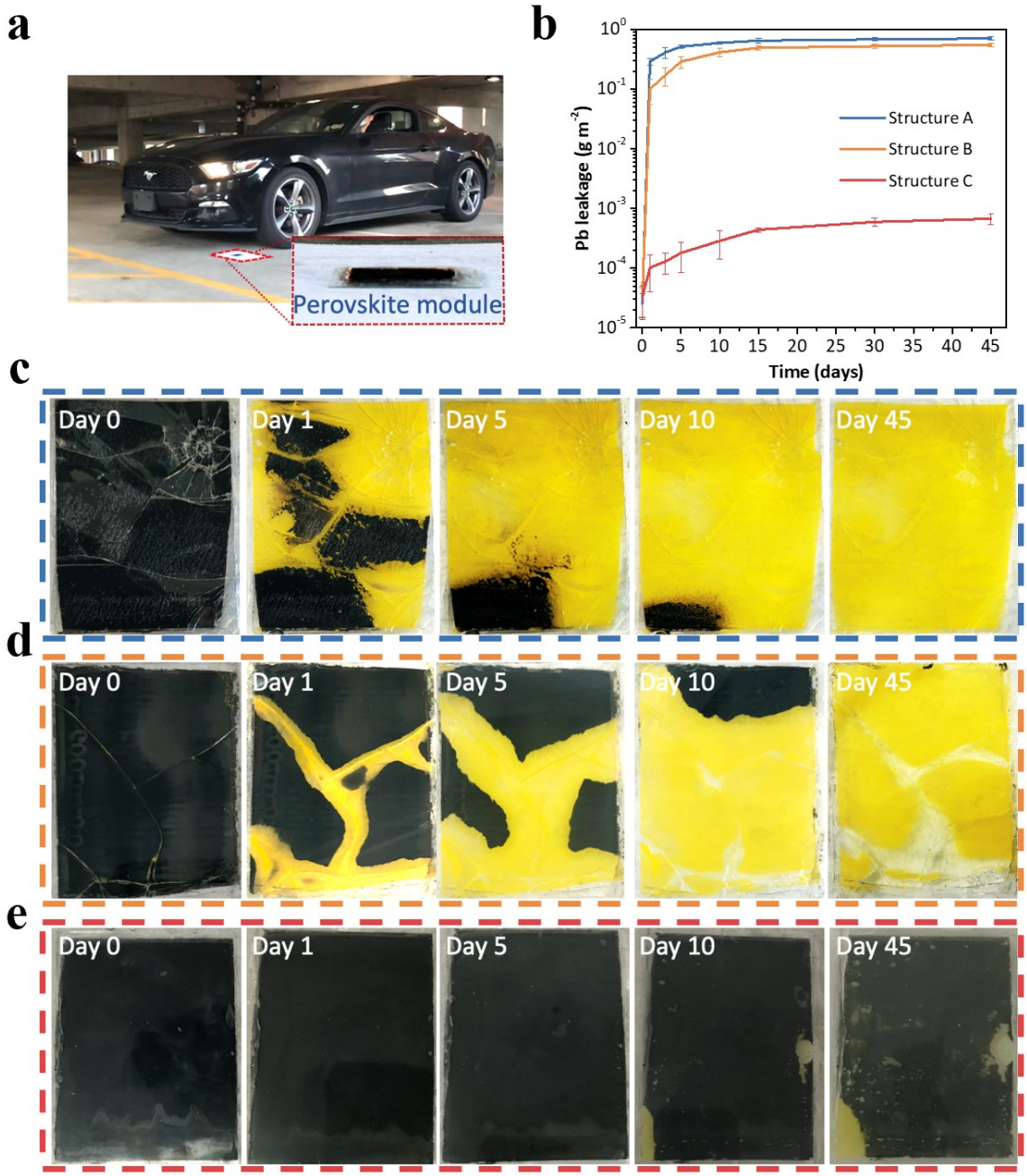

Fig. 4. Lead leakage test against getting run over by a car. a, image of car rolling on encapsulated perovskite films; **b**, water soaking test results of broken perovskite films; **c-e**, evolution images of damaged perovskite films with structure A(**c**), B(**d**), C (**e**) soaking in DI water. Photo credit: Xun Xiao, University of North Carolina Chapel Hill.

Table 1. Comparison of device performance with lead leakage-reduction structures in some recent reports

Ref.	Pb leakage reduction in standard hail test	Pb leakage reduction in extreme damaging test	Device efficiency without/with reduction structure	Device stability
(*21*)	96 %	N/A	19.69%/20.12%	N/A
(*18*)	N/A	N/A	N/A / 19.9%	12% efficiency loss @ 30 days in ambient condition
(*19*)	N/A	N/A	18.8%/22.02%	10% efficiency loss @ 1000 hours MPP tracking, 85 °C
(*20*)	98 %	N/A	19.5%/19.2%	N/A
(*17*)	>99%	N/A	N/A	N/A
This work	>99.9%	>99% @ car rolling over	22.45%/22.87%	4.8% efficiency loss @ 1000 h Damp Heat; 3.9 % efficiency loss @ 210 cycles of Temperature Cycling

Supplementary Materials

Please use the *Science Advances* template to format your Supplementary Materials.